scattering in $[Cr_2(OH)(NH_3)_{10}]Cl_5 \cdot H_2O$.[38] The failure of standard theoretical models to fit experimental magnetic susceptibility data for $(C_7H_7NH_3)_2MnCl_4$, $(C_7H_7NH_3)MnBr_4$,[39] and $Cu(n\text{-}C_3H_7nso)NO_3$[40,41] has been explained as a result of an increase in exchange coupling with decreasing temperature.

A decrease of the exchange integral with a decrease in temperature was determined by EPR in $[N(n\text{-}Bu)_4]_2[Cu(mnt)_2]$.[42] The exchange integral in this compound is nearly constant above 200 K ($\sim$0.04 cm^{-1}), below which J' decreases strongly with temperature. Magnetic susceptibility measurements on binuclear copper(II) cryptates yield $2J = -57$ cm^{-1} above 50 K, but exchange coupling decreases rapidly at low temperatures.[43]

The decrease of interdimer superexchange interaction with temperature in these crystals probably is a result of dynamical crystal lattice properties. Exchange interactions are expected to be proportional to overlap integrals between atomic orbitals in the superexchange pathways. The overlapping of orbitals is modulated by thermal lattice vibrations and depends on the average amplitude of atomic displacements, which are temperature dependent. The mean-square displacement of atoms $\langle\mu^2\rangle$ varies linearly[44,45] with temperature in the high-temperature region, where coth $(\hbar\omega/2kT) \approx 2kT/\hbar\omega$ ($\hbar\omega$ is the energy of a normal mode of a lattice vibration). Thus, the temperature dependence of interdimer exchange can be related to $\langle\mu^2\rangle$, as has been observed for the g factor in a HgSe:Mn^{2+} single crystal[33] and for the isotropic hyperfine splitting of Cu^{II} and vanadyl complexes in solutions.[46,47]

Conclusions

The compounds presented in this paper have similar crystal and molecular structures and magnetic properties. The differences in the intradimer exchange coupling in $Cu_2Cl_8^{4-}$ units reflect small differences in chloride bridge geometry. The electronic structures of individual Cu(II) complexes in the three compounds have ground states containing the mixed orbitals $\psi_{gs} = 0.98(d_{x^2-y^2}) + 0.2(d_{z^2})$. The main differences observed in the EPR spectra of these compounds result from differences in interdimer exchange coupling. Interdimer coupling is about 3 orders of magnitude smaller than intradimer coupling, but it produces a broadening and a shift of the EPR lines.

The temperature behavior of the interdimer exchange integral J' in these compounds reflects dynamical properties of the crystal lattice. In general, however, the problem of the temperature dependence of the exchange integral is complicated, and there are differences both in the sign and in the shape of dJ/dT in the systems that have been studied. The crystal lattice contraction effect on dJ/dT and a phonon modulation of orbital overlapping can produce effects of opposite sign. An anisotropy in the lattice contraction and more than one superexchange pathway can complicate the situation even more. Significant effects are produced by exchange elasticity phenomena,[43] where competition between elastic crystal energy and exchange coupling can determine an equilibrium state of the crystal lattice or molecular structure of a paramagnetic cluster. In crystals where the ground state of the cluster is diamagnetic, as it is in the case of antiferromagnetically coupled Cu(II) dimers, the interdimer exchange coupling is expected to be proportional to the probability that nearest neighbors are in excited paramagnetic states.[48,49] This dependence can influence J' values for temperatures lower than the singlet–triplet splitting, although definite experimental evidence does not exist to support this contention.

Acknowledgment. This research was supported by the National Science Foundation (Grant No. CHE 8308129) and the Petroleum Research Fund, administered by the American Chemical Society.

Registry No. I, 28852-88-2; II, 86751-15-7; III, 86959-84-4.

Supplementary Material Available: Listings of hydrogen atom positional parameters, anisotropic thermal parameters, and observed and calculated structure factors (45 pages). Ordering information is given on any current masthead page.

(37) Beutler, A.; Güdel, H. U.; Snellgrove, T. K.; Chapuis, G.; Schenk, K. *J. Chem. Soc., Dalton Trans.* **1979**, 983.
(38) Güdel, H. U.; Furrer, A. *Mol. Phys.* **1977**, *33*, 1335.
(39) Groenendijk, H. A.; Duyneveldt, A. J.; Willett, R. D. *Physica B+C (Amsterdam)* **1979**, *98B+C*, 53.
(40) Mikuriya, M.; Okawa, H.; Kida, S. *Bull. Chem. Soc. Jpn.* **1982**, *54*, 2979.
(41) Nakatsuka, S.; Osaki, K.; Uryu, N. *Inorg. Chem.* **1982**, *21*, 4332.
(42) Plumlee, K. W.; Hoffman, B. M.; Ibers, J. A.; Soos, Z. G. *J. Chem. Phys.* **1975**, *63*, 1926.
(43) Kahn, O.; Morgenstern-Badarau, I.; Audiere, J. P.; Lehn, J. M.; Sullivan, S. A. *J. Am. Chem. Soc.* **1980**, *102*, 5935.
(44) Willis, B. T.; Pryor, A. W. "Thermal Vibrations in Crystallography"; Cambridge University Press: New York, 1975.
(45) Shrivastava, K. N. *J. Phys. C.* **1982**, *15*, 3869.
(46) Baranov, D. G.; Zhytnikov, R. A.; Melnikov, N. I. *Phys. Status Solidi* **1969**, *33*, 463.
(47) Bylinskaya, L. A.; Kozyrev, B. M.; Ovchinnikov, I. V. *Magn. Reson. Relat. Phenom., Proc. Congr. Ampere* **1977**, *17*, 1000.
(48) Soos, Z. G. *J. Chem. Phys.* **1966**, *44*, 1729.
(49) McGregor, K. T.; Soos, Z. G. *Inorg. Chem.* **1976**, *15*, 1976.

Contribution from the School of Chemistry,
University of New South Wales, Kensington, NSW 2033, Australia

c-$Ni_8(SCH_2COOEt)_{16}$, a Receptive Octagonal Toroid

IAN G. DANCE,* MARCIA L. SCUDDER, and RODNEY SECOMB

Received July 2, 1984

The red compound $Ni(SCH_2COOEt)_2$, prepared by interaction of ethyl 2-mercaptoacetate with nickel salts in basic solution, is unusually soluble in a variety of inert solvents. The crystals contain cyclic molecules $Ni_8(SCH_2COOEt)_{16}$ in which eight NiS_4 rectangular coordination planes (Ni–S = 2.19 Å; S–Ni–S = 82.4, 98.3°) constitute an octagonal prism. The approximate molecular symmetry is C_{8h} for the Ni_8S_{16} core and D_{4d} when the axial and equatorial S–C bonds are included, while the array of externally pendant ligand tails is asymmetric. The Ni···Ni diameters of the toroidal molecule range from 7.6 to 8.3 Å; S···S diameters range from 8.0 to 9.6 Å. This allows sufficient space for inclusion (van der Waals or coordinative) of small molecules, and the tail of one axial ligand returns to enter the octagon with the ethyl group on the toroid axis and weak ester oxygen coordination to two adjacent nickel atoms (O–Ni = 3.0 Å). Inclusion of added species has not been detected. The detailed dimensions of the metal coordination and the hinged bridge in this first example of a cyclic $M_8(SR)_{16}$ molecule are evaluated in comparison with those of known $M_6(SR)_{12}$ and $M_4(SR)_8$ cyclic molecules. Crystal data: space group $P\bar{1}$, a = 13.367 (2) Å, b = 29.500 (3) Å, c = 29.818 (3) Å, α = 61.64 (1)°, β = 81.46 (1)°, γ = 81.35 (1)°, Z = 4, d_{obsd} = 1.56 g cm^{-3}, d_{calcd} = 1.55 g cm^{-3}, R = 0.088 for 8997 observed reflections.

Introduction

Compounds $M(SR)_2$ of the metals Ni, Pd, and Pt where R does not contain solubilizing functions are generally insoluble in inert solvents. Accordingly, one-dimensionally nonmolecular structures were proposed for these compounds by Jensen[1] in 1944, and have been assumed since, but have not been confirmed by diffraction

(1) Jensen, K. A. *Z. Anorg. Allg. Chem.* **1944**, *252*, 227.

0020-1669/85/1324-1201$01.50/0

analysis. In the period since 1965 several soluble crystalline forms of $M(SR)_2$ have been prepared by various methods,[2,3] and diffraction analyses have revealed the occurrence of the hexagonal molecular cycles $M_6(SR)_{12}$ (**1**) in the compounds $Ni_6(SEt)_{12}$,[4] $Ni_6(SCH_2CH_2OH)_{12}$,[5] $Pt_6(SPr)_{12}$,[6] and $Pd_6(SCH_2CH_2OH)_{12}$.[5,7] Cycle **1**, sometimes dubbed the "tiara" structure and proposed

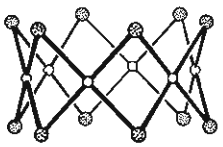

1

as a monomolecular inclusion host,[4] contains six edge-sharing coordination planes, each approximately square.

We have examined the Ni complex of the substituted thiolate ligand ethyl 2-mercaptoacetate and find it to be very soluble in a variety of inert media. The crystals contain cyclic octagonal molecules **2**, with eight linked square-planar segments and only

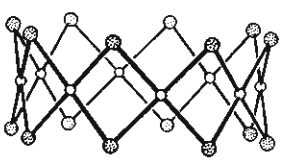

2

M–SR coordination. All ligand substituent chains are externally pendant except one that enters and occupies the large central hole. We have assessed the possibility that additional small molecules may be included or coordinated within the central cavity but have not yet found evidence for such behavior, possibly because the hole is blocked by the reentrant ligand.

The square cyclic structure $Ni_4(SR)_8$ (**3**) was recently reported for the complex in which SR is *N*-methylpiperidine-4-thiolato.[8]

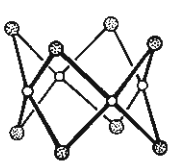

3

This paper describes the chemistry and structure of the $Ni_8(SCH_2COOEt)_{16}$ octagonal toroid and examines the differences in molecular structure between hexagonal **1**, octagonal **2**, and square **3**.

Experimental Section

Commercial ethyl 2-mercaptoacetate was used as received.

Preparation of $Ni_8(SCH_2COOEt)_{16}$. A solution of ethyl 2-mercaptoacetate (3.6 g, 30 mmol) and tributylamine (5.4 g, 30 mmol) in propanol (50 mL) was treated under nitrogen with a solution of $Ni(NO_3)_2 \cdot 6H_2O$ (4.5 g, 15 mmol) in propanol (30 mL). The resulting intensely red solution was allowed to stand first at room temperature and then at 0 °C. The red-black crystalline product was collected, washed with cold propanol and water, and vacuum dried (yield 4.0 g). This compound is soluble in acetone, acetonitrile, ethyl acetate, carbon disulfide, diethyl ether, benzene, toluene, dichloromethane, chloroform, and carbon tetrachloride. It is soluble in cold methanol and ethanol but dissolves in propanol and pentanol only when hot. It is not soluble in water. The crystals used for diffraction studies were long prisms grown from methanol/propanol.

Table I. Crystallographic Data for $Ni_8(SCH_2COOEt)_{16}$

formula, formula mass	$Ni_8S_{16}C_{64}O_{32}H_{112}$, 2376.3
cryst faces	{011}, {110}
space group	$P\bar{1}$
a/Å	13.367 (2)
b/Å	29.500 (3)
c/Å	29.818 (3)
α/deg	61.64 (1)
β/deg	81.46 (1)
γ/deg	81.35 (1)
V/Å^3	10189 (4)
temp/°C	21
d_{obsd}/g cm^{-3}	1.56
Z	4
d_{calcd}/g cm^{-3}	1.55
radiation, λ/Å	Cu Kα, 1.5418
μ/cm^{-1}	51.7
cryst dimens/mm	0.09 × 0.18 × 0.39
scan mode	$\theta/2\theta$
$2\theta_{max}$/deg	100
no. of intens measmts	14 525
criterion for obsd reflcn	$I/\sigma(I) > 2.58$
no. of indep obsd reflcns	11 217
limitation of data	$(\sin\theta)/\lambda > 0.25$
no. of reflcns (m) in final refinement	8997
R	0.088
R_w	0.093
n, $s = [\Sigma w\lvert\Delta F\rvert^2/(m-n)]^{1/2}$	453, 2.23
max, min transmission coeff	0.660, 0.212

Anal. Calcd for $[NiS_2C_8H_{14}O_4]_8$: C, 32.36; H, 4.72. Found: C, 32.79; H, 4.75. Mp: 95 °C.

The red color of solutions of $Ni_8(SCH_2COOEt)_{16}$ is changed to a less intense brown in the presence of large excesses of ligands pyridine and 2-methylpyridine.

Attempted cocrystallization experiments used $N_8(SCH_2COOEt)_{16}$ with the following compounds/solvents, without evidence (IR) for cocrystallization: $[MoS_4]^{2-}$ (cations Me_4N^+, $EtPh_3P^+$)/CH_3CN, NaI/acetone, Me_4NCl/MeOH, S_8/CS_2, I_2/acetone/cyclohexane, Ph_3P/various solvents, naphthalene/CH_3CN.

Crystallography. Photographic examination revealed no lattice symmetry. Unit cell dimensions were derived from diffractometer-centered reflections, by using Cu Kα radiation and a Siemens diffractometer. Crystallographic data, obtained by procedures already described,[9] are listed in Table I. Corrections for absorption and for intensity decay due to radiation damage were applied.

Direct methods applied with MULTAN80 (500 E's without structural information incorporated in the normalization) automatically yielded all 48 Ni and S atoms of the two molecules in the asymmetric unit. Further atom location proceeded by Fourier methods: many of the peripheral atoms were poorly defined, and one of the 240 non-hydrogen atoms in the asymmetric unit could not be found. Scattering factors including real and imaginary corrections for the anomalous dispersion of Ni and S were taken from ref 10. Least-squares refinements, based on F, incorporated only the 8997 observed data with $(\sin\theta)/\lambda > 0.25$, mainly to reduce the magnitude of the computing. No hydrogen atoms were included. The 239 non-hydrogen atoms were refined, with anisotropic thermal parameters for Ni and S atoms only. In the final cycle, the positions of all 48 Ni and S atoms along with those of the 32 α-carbon atoms C1 were refined by full-matrix least squares.

The atom-labeling scheme, which uses postscripts A and B to distinguish the two independent molecules in the asymmetric unit, is as follows: Nip, p = 1, 8; Spq and Sqp bridge Nip and Niq, with the eight atoms Spq, $p < q$, coplanar; ligand chains are Spq–C1pq–C2pq(–O1pq)–O2pq–C3pq–C4pq. The correspondence of p and q in the two molecules reflects close correspondences of geometrical detail and ligand configuration. Atomic coordinates are given in Table II, and thermal parameters are deposited;[11] rms displacements, averaged for chemically equivalent atoms, are Ni = 0.003, S = 0.005, C1 = 0.02, C2 = 0.03, O1 = 0.02, O2 = 0.03, C3 = 0.06, C4 = 0.06 Å. The lower accuracy of positions of the atoms at the ends of the ligand chains is shown also by the residual peaks in the final difference electron density map. The largest peaks, up to 2.5 e Å^{-3}, were near the peripheral atoms, and there were also peaks up to 1.5 e Å^{-3} in the vicinity of Ni atoms. One reason for the low

(2) Hayter, R. G.; Humiec, F. S. *J. Inorg. Nucl. Chem.* **1964**, *26*, 807.
(3) Abel, E. W.; Crosse, B. C. *J. Chem. Soc. A* **1966**, 1377.
(4) Woodward, P.; Dahl, L. F.; Abel, E. W.; Crosse, B. C. *J. Am. Chem. Soc.* **1965**, *87*, 5251.
(5) Gould, R. O.; Harding, M. M. *J. Chem. Soc. A* **1970**, 875.
(6) Kunchur, N. R. *Acta Crystallogr., Sect. B* **1968**, *B24*, 1623.
(7) Taylor, R. M. Ph.D. Thesis, University of Edinburgh, 1967.
(8) Gaete, W.; Ros, J.; Solans, X.; Font-Altaba, M.; Briansó, J. L. *Inorg. Chem.* **1984**, *23*, 39.
(9) Dance, I. G. *Inorg. Chem.* **1981**, *20*, 1487.
(10) "International Tables for X-ray Crystallography"; Kynoch Press: Birmingham, England, 1974; Vol IV, Tables 2.2A and 2.3.1.
(11) See paragraph at end of paper regarding supplementary material.

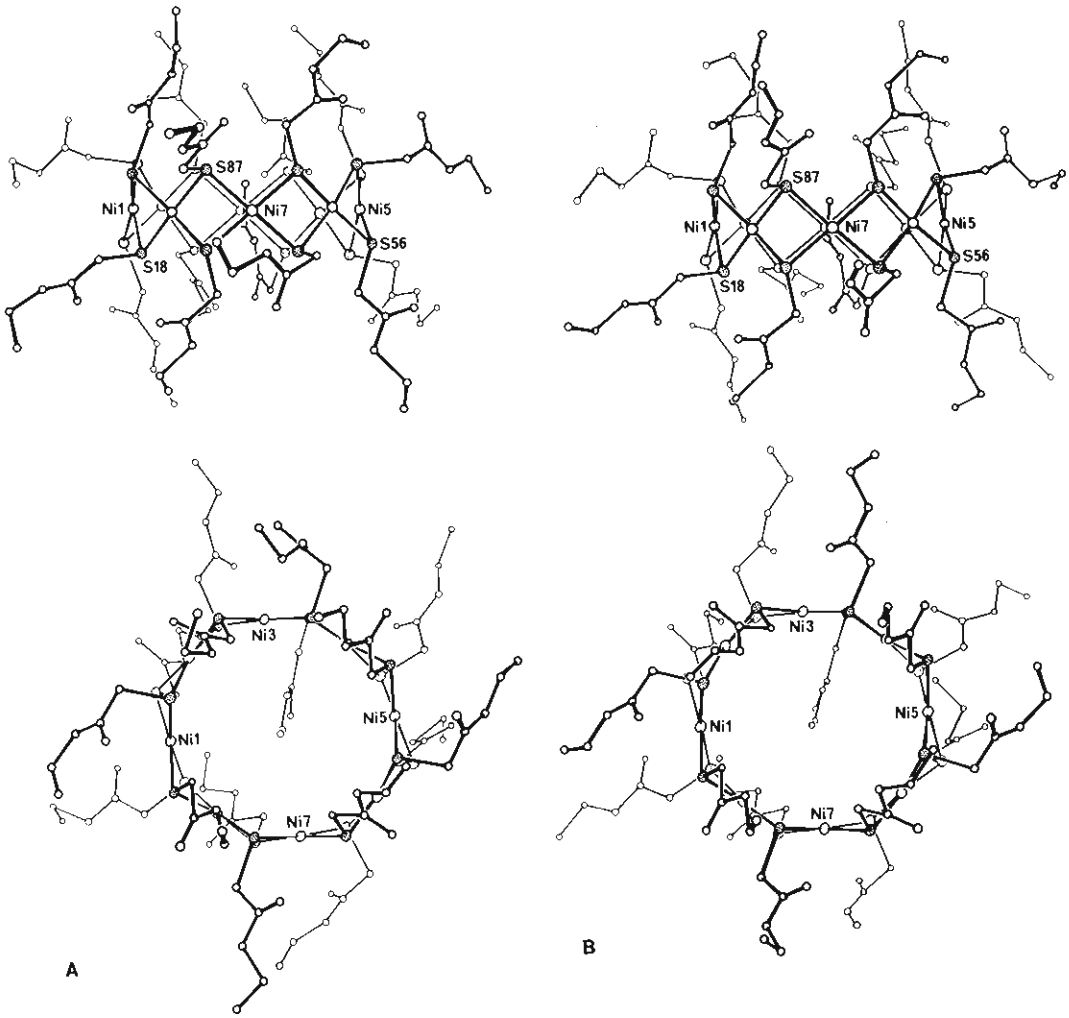

Figure 1. Comparable views of $Ni_8(SCH_2COOEt)_{16}$ molecules A and B, parallel and perpendicular to the toroid axis. Atoms Spq, $p > q$, occur in the upper S octagon.

accuracy of the light-atom determination was the radiation damage to the crystal during the data collection.

In view of the lattice pseudosymmetry that was apparent in the completed crystal structure, possible transformations of the lattice to higher symmetry space groups were investigated. In all cases the discrepancies in transformed lattice dimensions were well beyond experimental error, and there were clear differences in the intensities of supposedly equivalent reflections. The definite differences between the conformations and dimensions of the two molecules in the asymmetric unit further support the conclusion that the space group is in fact $P\bar{1}$.

Results and Discussion

Formation. $Ni_8(SCH_2COOEt)_{16}$ is easily prepared from mixtures of the thiol ligand, base, and metal salt and, unlike compounds $Ni(SR)_2$ with unfunctionalized thiols, is readily soluble in solvents such as acetone, acetonitrile, chlorocarbons, and the lower alcohols. This high solubility is consistent with the molecular structure in the crystal phase and with the elongated polar substituent chains.

There is no evidence of the equilibrium or nonequilibrium formation of sparingly soluble phases or of compounds $[Ni(SCH_2COOEt)_2]_p$, either molecular with $p \neq 8$ or nonmolecular with $p \rightarrow \infty$. In the $Ni(SEt)_2$ system the soluble molecular form $Ni_6(SEt)_{12}$ is thermodynamically unstable with respect to uncharacterized polymers.[3,4] In the $Ni^{2+}/^{-}SCH(CH_3)CH_2OH$ system, in water, $Ni_6(SR)_{12}$ molecules predominate at 25 °C, but at 75 °C, pH titration data indicate equilibria involving a series of open-chain complexes $Ni[Ni(SR)_2]_p^{2+}$, with an average value of $p \approx 30$.[7] With the sulfonated ligand $^{-}SCH_2CH_2SO_3^{-}$, nickel forms complexes that are very soluble in water.[12]

(12) Dance, I. G.; Landers, A. E., unpublished results.

Molecular Structure. Two very similar but crystallographically independent cyclic molecules of $Ni_8(SCH_2COOEt)_{16}$ occur in the crystals. Each molecule is composed of an approximate octagon of nickel atoms, with two doubly bridging thiolate ligands between each adjacent pair such that the metal coordination is approximately square planar. Alternatively, with emphasis on the metal coordination polygons, the molecule is described as an octagonal cycle of eight square planes linked via opposite edges to form an octagonal prism. The molecule is a segmented octagonal toroid.

Figure 1 shows comparable views of the two molecules parallel and perpendicular to the toroid axis. It can be seen that each Ni_8 octagon is approximately planar, with larger and approximately planar S_8 octagons above and below. However Figure 1 also shows that there are distortions within the Ni_8S_{16} core of each molecule and that the ligand chains take a variety of conformations. At each sulfur atom there are two possible directions for the S–C1 bond, which may be approximately axial or equatorial to the toroid. In fact these bond configurations alternate around the S_8 octagons, such that the 16 S–C1 vectors are approximately related by the operations of two coaxial S_8 ($\bar{8}$) symmetry elements. Therefore, although the complete molecule does not approximate to any symmetry, the central regions approach high symmetry. The most realistic idealization involves the 40 atoms of $Ni_8(S–C1)_{16}$, with the symmetry of point group D_{4d}.

It is remarkable that the various distortions from the D_{4d} idealization are very similar in the two crystallographically independent molecules. There are close correspondences of geometrical detail and similarities in the positions of some but not all of the pendant ligand substituents. In both molecules the tail of one axial ligand enters the toroid cavity, while the remainder extend away from the Ni_8S_{16} core. In Figure 1 the molecules are

Table II. Atomic Coordinates

	molecule A			molecule B		
atom	*x*	*y*	*z*	*x*	*y*	*z*
Ni1	0.6082 (2)	0.1684 (1)	0.0993 (1)	−0.0456 (2)	0.5038 (1)	0.2633 (1)
Ni2	0.6793 (2)	0.0637 (1)	0.1845 (1)	−0.1032 (2)	0.4009 (1)	0.3481 (1)
Ni3	0.5638 (2)	−0.0294 (1)	0.2519 (1)	0.0227 (2)	0.3130 (1)	0.4279 (1)
Ni4	0.3402 (2)	−0.0563 (1)	0.2686 (1)	0.2485 (2)	0.2850 (1)	0.4548 (1)
Ni5	0.1309 (2)	−0.0042 (1)	0.2325 (1)	0.4501 (2)	0.3289 (1)	0.4118 (1)
Ni6	0.0588 (2)	0.0995 (1)	0.1541 (1)	0.5046 (2)	0.4307 (1)	0.3237 (1)
Ni7	0.1811 (2)	0.1908 (1)	0.0791 (1)	0.3781 (2)	0.5247 (1)	0.2488 (1)
Ni8	0.4038 (2)	0.2172 (1)	0.0568 (1)	0.1541 (2)	0.5542 (1)	0.2253 (1)
S12	0.7261 (3)	0.1074 (2)	0.1031 (1)	−0.1601 (4)	0.4811 (2)	0.3280 (2)
S21	0.6473 (3)	0.1421 (2)	0.1776 (2)	−0.0798 (4)	0.4326 (2)	0.2645 (2)
S23	0.6794 (3)	−0.0115 (2)	0.1868 (1)	−0.0956 (4)	0.3732 (2)	0.4299 (1)
S32	0.6502 (3)	0.0184 (2)	0.2673 (1)	−0.0678 (4)	0.3182 (2)	0.3695 (2)
S34	0.4840 (4)	−0.0802 (2)	0.2370 (2)	0.1050 (4)	0.3062 (3)	0.4893 (2)
S43	0.4389 (3)	−0.0425 (2)	0.3123 (1)	0.1478 (4)	0.2589 (2)	0.4214 (2)
S45	0.2400 (3)	−0.0605 (2)	0.2183 (2)	0.3500 (4)	0.3190 (2)	0.4805 (2)
S54	0.1952 (3)	−0.0416 (2)	0.3064 (1)	0.3917 (4)	0.2565 (2)	0.4280 (2)
S56	0.0393 (3)	0.0219 (2)	0.1679 (1)	0.5348 (4)	0.3903 (2)	0.4042 (1)
S65	0.0459 (3)	0.0628 (2)	0.2381 (1)	0.5214 (3)	0.3510 (2)	0.3336 (1)
S76	0.0571 (3)	0.1797 (2)	0.1389 (1)	0.5040 (4)	0.4726 (2)	0.2404 (1)
S67	0.1092 (3)	0.1318 (2)	0.0727 (1)	0.4526 (4)	0.5073 (2)	0.3171 (2)
S87	0.2649 (3)	0.2419 (2)	0.0917 (2)	0.2928 (4)	0.5335 (2)	0.1871 (2)
S78	0.2953 (2)	0.2083 (2)	0.0140 (1)	0.2612 (4)	0.5847 (2)	0.2504 (2)
S18	0.5423 (3)	0.1844 (2)	0.0291 (1)	0.0156 (4)	0.5656 (2)	0.2705 (2)
S81	0.5121 (3)	0.2388 (2)	0.0893 (2)	0.0458 (4)	0.5351 (2)	0.1903 (1)
C112	0.6997 (15)	0.0751 (8)	0.0668 (6)	−0.1411 (19)	0.4999 (10)	0.3735 (8)
C212	0.7819	0.0335	0.0690	−0.2186	0.4839	0.4193
O112	0.8667	0.0288	0.0809	−0.3009	0.4751	0.4190
O212	0.7469	0.0062	0.0547	−0.1918	0.4841	0.4559
C312	0.8186	−0.0362	0.0561	−0.2660	0.4688	0.4988
C412	0.7782	−0.0597	0.0288	−0.2344	0.4854	0.5302
C121	0.7726 (15)	0.1677 (8)	0.1667 (6)	−0.2106 (14)	0.4506 (7)	0.2417 (6)
C221	0.7657	0.2223	0.1361	−0.2077	0.4916	0.1918
O121	0.7144	0.2530	0.1483	−0.1550	0.4837	0.1546
O221	0.8182	0.2385	0.0914	−0.2569	0.5356	0.1848
C321	0.8212	0.2966	0.0607	−0.2475	0.5721	0.1315
C421	0.7790	0.3114	0.0196	−0.3008	0.6102	0.1355
C132	0.5717 (16)	0.0562 (8)	0.2964 (7)	0.0121 (15)	0.3065 (8)	0.3223 (6)
C232	0.6248	0.0821	0.3103	−0.0497	0.3082	0.2815
O132	0.7147	0.0849	0.3071	−0.1386	0.3080	0.2853
O232	0.5675	0.1113	0.3273	−0.0006	0.3193	0.2398
C332	0.6145	0.1429	0.3453	−0.0445	0.3151	0.2002
C432	0.6278	0.1022	0.4084	−0.0660	0.3665	0.1706
C123	0.7929 (15)	−0.0533 (8)	0.2149 (6)	−0.2088 (14)	0.3382 (8)	0.4613 (6)
C223	0.7989	−0.1039	0.2183	−0.1978	0.3060	0.5137
O123	0.7538	−0.1149	0.1961	−0.1723	0.3210	0.5425
O223	0.8670	−0.1338	0.2457	−0.2162	0.2576	0.5325
C323	0.8933	−0.1893	0.2496	−0.2236	0.2122	0.5915
C423	0.9931	−0.2130	0.2550	−0.3106	0.2009	0.6039
C134	0.4772 (18)	−0.0524 (9)	0.1687 (8)	0.1130 (19)	0.3715 (10)	0.4803 (8)
C234	0.4367	−0.0009	0.1452	0.1485	0.4050	0.4334
O134	0.4114	0.0219	0.1011	0.1515	0.4491	0.4382
O234	0.4203	0.0277	0.1689	0.1655	0.3986	0.3949
C334	0.3758	0.0820	0.1476	0.1996	0.4306	0.3427
C434	0.3577	0.0964	0.1880	0.2170	0.4050	0.3162
C143	0.4738 (24)	−0.1088 (13)	0.3631 (10)	0.1242 (17)	0.1942 (9)	0.4776 (7)
C243	0.5620	−0.1101	0.3849	0.0676	0.1651	0.4636
O143	0.6457	−0.1263	0.3744	0.0364	0.1769	0.4260
O243	0.5399	−0.0973	0.4203	0.0529	0.1219	0.5061
C343	0.5641	−0.0662	0.3970	−0.0257	0.0877	0.5029
C443	0.6436	−0.0697	0.4437	0.0104	0.0522	0.5244
C145	0.1835 (17)	−0.1236 (9)	0.2555 (7)	0.4113 (17)	0.2654 (9)	0.5341 (7)
C245	0.2531	−0.1647	0.2479	0.3583	0.2589	0.5823
O145	0.3036	−0.1585	0.2107	0.2699	0.2713	0.5899
O245	0.2409	−0.2082	0.2870	0.4114	0.2310	0.6215
C345	0.2955	−0.2551	0.2820	0.3642	0.2183	0.6769
C445	0.3089	−0.2966	0.3355	0.4371	0.2246	0.6981
C154	0.2023 (15)	0.0036 (8)	0.3317 (6)	0.3850 (17)	0.2504 (9)	0.3697 (7)
C254	0.2423	−0.0222	0.3821	0.3463	0.2013	0.3797
O154	0.2462	−0.0678	0.4101	0.3369	0.1649	0.4193
O254	0.2760	0.0128	0.3911	0.3222	0.2077	0.3378
C354	0.3219	−0.0164	0.4441	0.2881	0.1567	0.3432
C454	0.3569	0.0197	0.4474	0.3118	0.1540	0.2958
C165	−0.0826 (15)	0.0422 (8)	0.2607 (6)	0.6577 (14)	0.3270 (8)	0.3429 (6)
C265	−0.0804	−0.0018	0.3119	0.6664	0.2744	0.3739

Table II (*Continued*)

atom	molecule A			molecule B		
	x	y	z	x	y	z
O165	−0.0548	0.0000	0.3493	0.6438	0.2413	0.3649
O265	−0.0897	−0.0459	0.3159	0.6958	0.2600	0.4198
C365	−0.0792	−0.0917	0.3660	0.7216	0.2058	0.4516
C465	−0.0808	−0.1353	0.3591	0.6497	0.1848	0.4829
C156	0.0979 (15)	0.0060 (8)	0.1179 (6)	0.4745 (16)	0.4247 (8)	0.4393 (7)
C256	0.0822	−0.0455	0.1272	0.5017	0.3975	0.4919
O156	0.0375	−0.0754	0.1621	0.5535	0.3593	0.5145
O256	0.1220	−0.0525	0.0897	0.4658	0.4253	0.5141
C356	0.1010	−0.1135	0.0954	0.4412	0.3981	0.5801
C456	0.0861	−0.1029	0.0536	0.3445	0.3934	0.5952
C176	0.0959 (15)	0.1866 (8)	0.1920 (7)	0.4675 (14)	0.4336 (7)	0.2144 (6)
C276	0.0110	0.1789	0.2305	0.5534	0.4032	0.2039
O176	−0.0791	0.1829	0.2275	0.6414	0.3988	0.2101
O276	0.0438	0.1726	0.2738	0.5153	0.3676	0.1940
C376	−0.0358	0.1680	0.3173	0.5916	0.3213	0.1917
C476	−0.0427	0.1228	0.3445	0.5912	0.2742	0.2388
C167	−0.0067 (15)	0.1669 (8)	0.0392 (6)	0.5601 (17)	0.5461 (9)	0.2932 (7)
C267	0.0304	0.2033	−0.0138	0.5232	0.6037	0.2769
O167	0.0772	0.1900	−0.0447	0.4808	0.6118	0.3097
O267	0.0247	0.2506	−0.0231	0.5216	0.6268	0.2355
C367	0.0819	0.2852	−0.0744	0.5662	0.6248	0.2155
C467	0.0652	0.3344	−0.0744			
C187	0.2362 (17)	0.3088 (9)	0.0407 (7)	0.3203 (16)	0.5967 (8)	0.1319 (7)
C287	0.1386	0.3340	0.0523	0.4143	0.5820	0.0978
O187	0.0950	0.3191	0.0927	0.4602	0.5461	0.1082
O287	0.1322	0.3799	0.0092	0.4217	0.6187	0.0558
C387	0.0245	0.4156	0.0098	0.5042	0.6193	0.0159
C487	0.0493	0.4623	−0.0347	0.4548	0.6050	−0.0037
C178	0.3331 (6)	0.1533 (9)	0.0017 (7)	0.2226 (19)	0.5800 (10)	0.3153 (8)
C278	0.4128	0.1644	−0.0426	0.1467	0.6233	0.3123
O178	0.4314	0.2050	−0.0751	0.1229	0.6614	0.2777
O278	0.4545	0.1198	−0.0373	0.1102	0.6072	0.3593
C378	0.5482	0.1225	−0.0783	0.0282	0.6477	0.3691
C478	0.5918	0.0740	−0.0602	−0.0442	0.6224	0.3901
C118	0.5921 (15)	0.2417 (8)	−0.0237 (7)	−0.0377 (19)	0.6275 (10)	0.2248 (8)
C218	0.6916	0.2323	−0.0463	−0.1341	0.6509	0.2396
O118	0.7355	0.1897	−0.0350	−0.1738	0.6302	0.2816
O218	0.7233	0.2727	−0.0855	−0.1542	0.6966	0.2015
C318	0.8345	0.2684	−0.1103	−0.2473	0.7257	0.2129
C418	0.8109	0.2607	−0.1509	−0.2610	0.7741	0.1636
C181	0.4638 (15)	0.2403 (8)	0.1512 (7)	0.0968 (17)	0.4852 (9)	0.1704 (7)
C281	0.3970	0.2890	0.1408	0.1577	0.5092	0.1175
O181	0.3919	0.3267	0.1035	0.1599	0.5530	0.0890
O281	0.3450	0.2795	0.1851	0.2148	0.4719	0.1149
C381	0.2651	0.3247	0.1831	0.2835	0.4958	0.0654
C481	0.2702	0.3292	0.2274	0.2956	0.4558	0.0574

Table III. Ni–S Bond Lengths[a,b]

indices p, q, r	molecule A				molecule B			
8, 1, 2	2.208	2.184	2.178	2.200	2.216	2.173	2.173	2.197
1, 2, 3	2.182	2.201	2.186	2.184	2.187	2.196	2.190	2.201
2, 3, 4	2.195	2.190	2.198	2.196	2.213	2.198	2.189	2.185
3, 4, 5	2.182	2.187	2.212	2.186	2.191	2.200	2.208	2.170
4, 5, 6	2.196	2.186	2.193	2.193	2.191	2.194	2.183	2.205
5, 6, 7	2.177	2.196	2.185	2.183	2.184	2.206	2.186	2.188
6, 7, 8	2.206	2.182	2.185	2.201	2.204	2.174	2.191	2.199
7, 8, 1	2.189	2.190	2.195	2.171	2.183	2.190	2.204	2.180

[a] In Å; the esd is 0.006 Å for all distances. [b] The horizontal sequence of entries for each molecule is Niq–Spq, Niq–Sqp, Niq–Sqr, Niq–Srq.

Table IV. S–Ni–S Angles[a,b]

indices p, q, r	molecule A				molecule B			
	θ_1		θ_2		θ_1		θ_2	
8, 1, 2	82.0	81.9	99.7	98.7	82.2	82.4	99.2	98.3
1, 2, 3	81.8	82.6	97.6	99.4	82.2	82.7	97.8	98.9
2, 3, 4	82.3	82.6	96.4	99.0	82.3	83.5	96.2	98.3
3, 4, 5	83.2	82.5	97.7	97.4	83.1	82.5	97.6	97.5
4, 5, 6	82.8	82.3	98.9	98.5	82.3	82.1	98.9	99.4
5, 6, 7	82.7	82.7	98.0	98.4	82.1	82.4	99.1	98.7
6, 7, 8	82.3	82.2	98.0	98.2	82.3	82.0	99.0	97.6
7, 8, 1	82.4	82.5	98.5	97.6	82.4	82.4	98.9	97.4

[a] In deg; the esd is 0.2° for all angles. [b] The horizontal sequence of entries for each molecule is Spq–Niq–Sqp, Sqr–Niq–Srq (both θ_1 of Figure 2), Spq–Niq–Sqr, Sqp–Niq–Srq (both θ_2 of Figure 2).

oriented to show these correspondences, and the Ni and S atom-numbering schemes for the two molecules also reflect this correspondence.

Tables III–V report bond distances,[13] angles, and other relevant geometrical properties defined in Figure 2. Statistical values[14] are as follows: Ni–S = 2.191 Å (64, 0.011 Å); S–Ni–S within Ni_2S_2 cycles (θ_1) = 82.4° (32, 0.4°); S–Ni–S = outside Ni_2S_2 cycles (θ_2) = 98.3° (32, 0.8°); Ni–S–Ni ϕ_{ax} = 88.5° (16, 1.6°), ϕ_{eq} = 87.8° (16, 1.7°); Ni–S–C_{ax} = 113.1° (28,[15] 1.1°); Ni–S–C_{eq} = 105.0° (32, 2.6°). It should be noted that there is no significant differentiation of the Ni–S–Ni ϕ angles according to the axial

(13) Mean ligand bond lengths are S–C1 = 1.84, C1–C2 = 1.46, C2–O1 = 1.19, C2–O2 = 1.28, O2–C3 = 1.54, and C3–C4 = 1.36 Å.

(14) Reported as the mean, with sample size and standard deviation of the *sample* in parentheses.

(15) The values for S34, which supports the anomalous reentrant ligand, are excluded.

Table V. Angles at Thiolate Sulfur Atoms[a]

sulfur atom	Ni–S–Ni, ϕ[b] molecule A	molecule B	β[c] molecule A	molecule B
	Axially Directed Ligands			
S12	88.6	87.1	31	34
S32	87.1	87.4	33	31
S34	90.7	91.1	26	25
S54	89.0	87.0	33	33
S56	85.2	87.1	35	33
S76	89.5	89.1	33	32
S78	89.8	89.5	32	35
S81	88.6	89.1	35	34
	Equatorially Directed Ligands			
S21	87.6	86.3	21	20
S23	86.9	87.3	25	20
S43	90.6	91.0	19	19
S45	88.0	86.1	22	23
S65	84.7	86.0	21	21
S67	88.8	88.4	21	24
S87	89.3	89.1	21	20
S18	87.4	87.3	22	22

[a] See Figure 2. [b] In deg; the esd is 0.2° for all angles. [c] The angle (in deg) between the S–C1 vector and the normal to the Ni–S–Ni plane; see Figure 2.

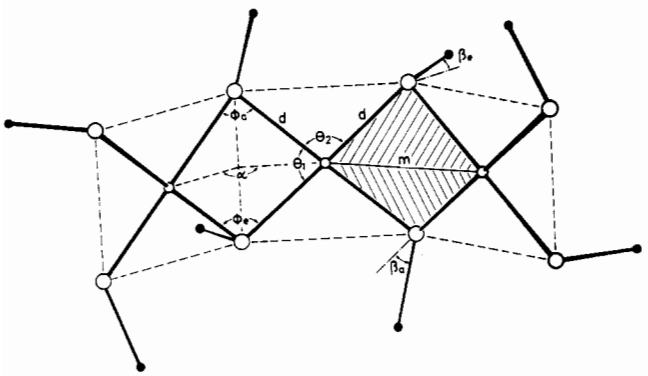

Figure 2. Definition of geometrical properties at the edge linkage of coordination planes and at the bridging S atoms. The small open circles are Ni atoms.

or equatorial configuration of the ligand but that there is a differentiation of the angles Ni–S–C and of the angle β of the S–C1 vector to the Ni–S–Ni plane: mean values[14] are 33.1° (14,[15] 1.4°) for β_{ax} and 21.3° (16, 1.7°) for β_{eq}.

Molecular planes are described in Table VI; the mean displacement of the nickel atoms from their coordination planes is only 0.02 Å. The contracycle dimensions reported in Table VII show that the core of each molecule is more closely approximated to symmetry C_{2v}, with mirror planes passing through S12, S56, S21, and S65 and through S34, S78, S43, and S87; the related distances are Ni1···Ni5 and Ni2···Ni6 (8.09, 8.34 Å (A); 8.17, 8.20 Å (B)), Ni3···Ni7 and Ni4···Ni8 (7.81, 7.59 Å (A); 7.72, 7.70 Å (B)), S23···S67 and S45···S18 (8.49, 7.97 Å (A); 8.33, 8.22 Å (B)), and S32···S76 and S54···S81 (8.98, 8.93 Å (A); 8.89, 9.07 Å (B)).

Figure 1 shows that one of the sixteen ligands, the one axially connected at S34 in both molecules, bends under the cycle and enters it between Ni3 and Ni4, such that the ester oxygen atom O2 is located close to the axial coordination position for both nickel atoms. The details of this entrance and the weak nickel coordination are shown in Figure 3. The O2–Ni3 and O2–Ni4 distances are 3.02 and 3.00 Å and 3.09 and 3.07 Å in molecules A and B, respectively. The ethyl group of this inserted ligand is positioned close to the center of the toroid and coaxial with it. Although the O2–Ni coordination is very weak, and does not cause any displacement of Ni3 or Ni4 from their S_4 coordination planes, it does have minor repercussions in the dimensions of the toroid: the angles β_{ax} at S34 are 26 and 25° for molecules A and B instead

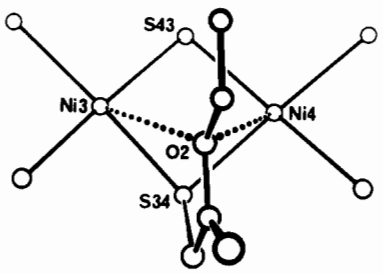

Figure 3. Distant coordination of Ni3 and Ni4 by the reentrant ligand.

of the average 33° for the remainder, and the angles α (see Figure 2) are 2 and 11° larger than the average of the remainder. A possible nonbonding influence of the inserted ligand is apparent in the lengths of the S12···S56 diagonals, which are extended by ca. 1 Å; this diagonal is bisected by the plane of the reentrant ligand. In fact, the reentrant ligand almost fills the cavity of the toroid: the appropriate sum of the van der Waals radii of the nickel or sulfur atoms (ca. 1.8 Å[16]) and of the ethyl group (ca. 2 Å) is ca. 7.6 Å, almost the diameter of the toroid.

If one ligand remains reentrant in the toroid in solution, it would effectively block inclusion of other small molecules.

Geometrical Comparison of c-$M_p(\mu\text{-}SR)_{2p}$ (p = 4, 6, 8). Toroidal molecules $Ni_p(\mu\text{-}SR)_{2p}$ are now known with four, six, and eight metal atoms, and in all cases the Ni_p polygon is exactly or virtually planar.[17] The obvious geometrical difference is the change of the dihedral angle between adjacent S_4 coordination planes: 90, 120, 135° for p = 4, 6, 8. However, this difference requires variation in the details of the stereochemistry at nickel and/or bridging thiolate, and we have examined these details in an attempt to discern the cause of the variation in toroid size. Relevant geometrical data, defined by Figure 2, are collected in Table VIII.

The angles α, θ_1, and ϕ are constrained by the relationship $\sin(\phi/2) = 2\sin(\alpha/2)\cos(\theta_1/2)$. Increase in the dihedral angle α between contiguous segments of the toroid can be absorbed by increase in ϕ and/or decrease in θ_1. Alternatively, as α decreases, the nickel atoms may be displaced outside their S_4 coordination planes. This latter effect occurs in the strained square toroid only. It can be seen from Table VIII that the angles θ_1 and θ_2 are unchanged with toroid size and that the systematic variation in stereochemistry is an increase in the angles ϕ at the bridging thiolate as the toroid expands. In view of the wide range of values (65–140°) known for M–S(R)–M angles in metal thiolates,[18,19] it appears unlikely that this factor could have substantial influence on toroid size. The correlation of decreasing pyramidality at sulfur with increasing M–S–M angle, which occurs generally in metal thiolates,[19] would here cause β to increase as ϕ and toroid size increase and reduce the difference between axial and equatorial ligands, which could then mutually interfere in large toroids.

It is probable that the smaller square toroid is a consequence of steric interference between adjacent piperidine rings[8] and that the choice among hexagonal, octagonal, and larger toroids is not based on the stereochemistry at nickel or bridging thiolate. We believe that larger toroids are unlikely to form unless there is a central occupant, either a guest molecule or reentrant ligand, which by weak coordination to the metal, or by van der Waals interactions, provides some mechanical stabilization.

Crystal Packing and Pseudosymmetry. The packing of the molecules in the lattice is shown in Figure 4. The toroid axes

(16) Dance, I. G.; Solstad, P. J.; Calabrese, J. C. *Inorg. Chem.* **1973**, *12*, 2161.
(17) A related compound is the cyclic trimetallic molecule $(S\text{--}S)_3Ni_3(PPh_3)_3$ where (S--S) is the chelating dithiolate ligand hexachloronaphthalene-1,2-dithiolate, but it is not considered here because the metal is five-coordinate and the molecular structure is constrained by the rigidity of the ligands: Bosman, W. P.; van der Linden, H. G. M. *J. Chem. Soc., Chem. Commun.* **1977**, 714.
(18) Dance, I. G.; Fitzpatrick, L. J.; Scudder, M. L. *J. Chem. Soc., Chem. Commun.* **1983**, 546.
(19) Dance, I. G.; Scudder, M. L., manuscript in preparation.

Table VI

Displacements[a] of Atoms from X_8 Octagonal Planes

plane, X	molecule	1	2	3	4	5	6	7	8
I, S above	A	22.7	−0.5	−7.4	−15.1	24.1	−4.2	−4.0	−15.6
	B	−24.5	2.4	8.5	14.3	−27.0	7.0	4.8	14.6
II, Ni	A	1.2	10.8	−1.9	−11.3	2.9	10.0	−2.4	−9.4
	B	−3.3	−10.0	0.3	11.1	−5.0	−9.6	4.3	9.0
III, S below	A	18.6	0.8	−3.8	−16.3	20.6	−2.5	−1.0	−16.5
	B	−19.4	1.2	4.1	15.4	−22.9	4.8	1.8	15.0

Angles[b] between Planes

I/II: 0.2 (A), 0.3 (B) II/III: 0.1 (A), 0.1 (B) I/III: 0.1 (A), 0.2 (B)

[a] In pm. [b] In deg.

Table VII. Intramolecular Nonbonded Distances[a]

	molecule A	molecule B		molecule A	molecule B
			Ni···Ni Diagonals		
Ni1···Ni5	8.090	8.176	Ni3···Ni7	7.805	7.734
Ni2···Ni6	8.332	8.191	Ni4···Ni8	7.601	7.708
			S···S Diagonals		
S12···S56	9.563	9.571	S34···S78	8.232	8.233
S21···S65	8.406	8.307	S43···S87	8.080	8.070
S23···S67	8.479	8.332	S45···S18	7.977	8.207
S32···S76	8.972	8.892	S54···S81	8.931	9.062
			Bridged Ni–Ni		
Ni1–Ni2	3.046	3.005	Ni5–Ni6	2.957	3.008
Ni2–Ni3	3.013	3.039	Ni6–Ni7	3.073	3.061
Ni3–Ni4	3.115	3.127	Ni7–Ni8	3.087	3.078
Ni4–Ni5	3.063	3.004	Ni8–Ni1	3.042	3.052

[a] In Å; esd's are 0.004 Å for Ni–Ni and 0.007 Å for S–S.

of the molecules are approximately parallel but are not coaxial and do not pass through the centers of symmetry. There are pseudo-twofold axes in the crystal lattice, parallel to *a*, relating molecules A and B.

Reactions with Additional Ligands and Potential Guest Molecules. Despite explorations with various potential guests and solvent systems, we have no evidence for cocrystallization by $Ni_8(SCH_2COOEt)_{16}$. Very large excesses of additional ligands such as pyridine are required to disrupt the square-planar coordination of nickel in this complex.

A polymetallic macrocyclic complex conceivably could include a small molecule held only by van der Waals forces or include a mono- or polyfunctional ligand coordinated to one or more metal atoms. The average diameter of $Ni_8(SR)_{16}$ is 7.9 Å. After subtraction of the van der Waals thickness of the toroid (2 × 1.8 Å[16]), a 4.3 Å diameter cylindrical shape is allowed for a van der Waals guest. This would effectively restrict inclusion to guest species with unbranched chains coaxial with the toroid.

An internally coordinating ligand could be a monodonor to one nickel atom, therefore being located asymmetrically within the toroid, or a polydonor to two or more nickel atoms, being located symmetrically about the toroid axis. Coordination bond distances

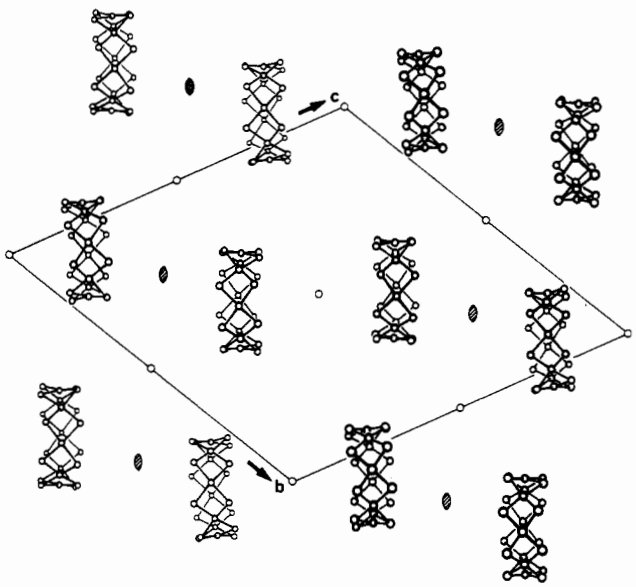

Figure 4. Lattice of Ni_8S_{16} cores projected along the *a* axis (13.4 Å), showing the inversion centers of space group $P\bar{1}$ and the pseudo-twofold axes (shaded ellipses) parallel to *a* through 0, $^1/_4$, $^1/_4$ and 0, $^3/_4$, $^3/_4$.

and van der Waals nonbonding contact distances within the toroid must be satisfactory. Taking into account the toroid flexibility (revealed by the Ni···Ni diameter range of 7.6–8.3 Å), we reach the following conclusions about the geometrical feasibility of internal coordination. Of the monodonor ligands, NH_3 is feasible but substituted homologues would be too large; XR_2 ligands are feasible when the R substituents are aligned with the toroid axis (the ester coordination of the reentrant ligand is in this category). As polydonor ligands oriented perpendicular to the toroid axis, azide and cyanate as bidonor ligands or nitrate as a tridonor ligand could be accommodated but squarate $\overline{OC-C(O)-C(O)-C(O)}$ with O···O diagonals of ca. 5 Å would be too large; ethylenediamine and 1,4-diazabicyclo[2.2.2]octane as bidonor ligands would permit suitable Ni–N distances, but the latter rigid ligand would have unsuitable van der Waals contacts between CH_2 and the

Table VIII. Dimensions[a] of Cyclic Molecules $Ni_p(SR)_{2p}$

R	*d*, Ni–S	*m*, Ni–Ni	ΔNi[b]	θ_1	θ_2	ϕ	ref
			Square Toroid; $p = 4$, $\alpha = 90°$				
N-Me-pip	2.21 (1)	2.67 (1)	0.22	81.2 (5)	98.2 (3)	74.3 (1)	8
			Hexagonal Toroids; $p = 6$, $\alpha = 120°$				
SCH_2CH_2OH	2.21 (2)	2.92 (1)	<0.06	82.6 (3)	97.5 (6)	82.9 (5)	6
Et	2.20	2.92	*c*	*c*	*c*	*c*	4
$(CH_2)_3NHMe_2$	2.20 (1)	2.93 (1)	*c*	*c*	*c*	*c*	*d*
			Octagonal Toroid; $p = 8$, $\alpha = 135°$				
CH_2COOEt	2.19 (1)	3.05 (4)	0.02	82.4 (4)	98.3 (8)	88 (2)	*e*

[a] In Å or deg. See Figure 2 for definition of symbols. Standard deviations quoted in parentheses are of the *sample*, not of individual values or of the mean. [b] Displacement of Ni from the S_4 coordination plane. [c] Not reported. [d] Unpublished results quoted in ref 8. [e] This work.

toroid. However it must also be borne in mind that the residual coordinating ability of nickel in $Ni_8(SCH_2COOEt)_{16}$ is very weak.

It is possible that by changing (increasing) the even number of segments the toroid size could change to accommodate guest molecules.

Conclusions

The inclusion of a molecular species, viz. an attached ester function, inside a macrocyclic polymetallic toroid $Ni_p(SR)_{2p}$, as suggested first by Dahl,[4] has been observed in $Ni_8(SCH_2COOEt)_{16}$, which is the first octagonal toroid.

The sizes of toroidal molecules $Ni_p(SR)_{2p}$ are not dominated by the stereochemistry at Ni or SR but can be determined by factors such as steric repulsions between ligand substituents (p = 4, four segments, square) or the van der Waals volume of an internal group (p = 8, eight segments, octagonal). In the absence of these factors, the hexagonal toroid with six segments is favored. It is possible that larger toroids with more than eight segments will occur as hosts for guest molecules of van der Waals diameter larger than the ethyl ester function.

Acknowledgment. We are grateful to Dr. R. O. Gould for access to unpublished results.[7] Kerry Edwards provided experimental assistance, and Don Craig collected the diffraction data. This research is funded by the Australian Research Grants Scheme.

Registry No. $Ni_8(SCH_2COOEt)_{16}$, 95045-16-2.

Supplementary Material Available: A tabulation of all atomic coordinates and thermal parameters and a listing of observed and calculated structure factors (49 pages). Ordering information is given on any current masthead page.

Contribution from the Department of Chemistry, University of the Witwatersrand, Johannesburg, South Africa

Crystallographic and Thermodynamic Study of Metal Ion Size Selectivity in the Ligand 1,4,7-Triazacyclononane-*N*,*N*′,*N*″-triacetate

MAGDALENA J. VAN DER MERWE, JAN C. A. BOEYENS,* and ROBERT D. HANCOCK*

Received July 3, 1984

The crystal structures of $H_3O[Ni(TACNTA)]$ (I) and $[CuCl(TACNTAH_2)]$ (II) are reported (TACNTA = 1,4,7-triazacyclononane-*N*,*N*′,*N*″-triacetate). I crystallizes in space group $P3c1$, with cell constants $a = b = 8.529$ Å, $c = 12.757$ Å, $\alpha = \gamma = 90°$, and $\beta = 95.30°$. The structure was refined to a conventional R factor of 0.0833. Of particular interest was the rather short Ni–N bond length of 2.04 Å. It was concluded that this represented the high packing efficiency of the ligand around Ni(II) rather than compression. Also of interest was the hydronium ion, which was found to be disordered in the structure. The complex is unique in crystallizing as an acid, rather than having protonated carboxylate groups, as is found for other complexes of poly(amino carboxylates). Structure II crystallizes in space group $P2_12_12_1$, with cell constants $a = 13.405$ Å, $b = 11.151$ Å, $c = 10.400$ Å, and $\alpha = \beta = \gamma = 90°$. A conventional R factor of 0.0616 was achieved. The coordination sphere around copper consists of two short Cu–N bonds of 2.07 and 2.04 Å and a long Cu–N bond of 2.38 Å. The unprotonated acetate is coordinated to the copper with a normal in-plane Cu–O length of 1.96 Å, while a protonated acetate occupies the axial site with a Cu–O length of 2.56 Å. The chloride occupies a position in the plane with a Cu–Cl length of 2.30 Å. The pK_a values of TACNTA were determined to be 11.41, 5.74, 3.16, and 1.71, and log K_1 with Mg(II) was found to be 8.93, and for Ca(II) 8.81, at 25 °C in 0.1 M $NaNO_3$. The relatively high stability of the Mg(II) complex as compared with Ca(II) is discussed in terms of the size selectivity of TACNTA toward small metal ions. The unusual stability of the Ni(III) complex of TACNTA is also discussed in terms of the preference of the ligand for small metal ions.

Introduction

A point of potential interest in the chemistry of the tetraaza nitrogen donor macrocycles is the size selectivity for metal ions expected from the cavities of fairly fixed size in the ligands.[1] If we examine the actual variation in log K_1 (the formation constant) for the macrocyclic tetraaza ligands and compare this with the variation for the open-chain analogous (Table I), we see that the variability in log K_1 is no greater in the macrocycles than the open-chain ligands. This rather surprising result reflects the flexibility in the macrocyclic ring recently demonstrated by molecular-mechanics (MM) calculation.[2] Thus, a ligand such as 12-aneN_4 (see Figure 1 for structures of ligands), which in its trans-III conformation[3] has a cavity size such that metal ions with an M–N bond length of 1.82 Å fit best, is able to adapt to larger metal ions by adopting the trans-I conformer, which has a best fit M–N length of 2.11 Å. Other means of relieving steric strain with too-large metal ions are by folding of the macrocycle (the trans-V conformer) or, in the case of Ni(II), by changing spin state from the high-spin to the smaller low-spin electronic configuration.

What is needed to overcome the flexibility of the largely two-dimensional macrocycle is a three-dimensional structure, in which metal ions cannot escape compression simply by folding the macrocycle or dropping down from high spin to low spin. Such a structure is provided by the title ligand, TACNTA (Figure 1), which coordinates octahedrally to the metal ion, offering no escape from compression as long as all the acetate groups remain coordinated. TACNTA was first synthesized by Takahashi and Takamoto,[4] and a crystallographic study of the Cr(III), Cu(II),

Table I. Formation Constants of Tetraaza Macrocycles and Their Open-Chain Analogues[a]

	ligands			
	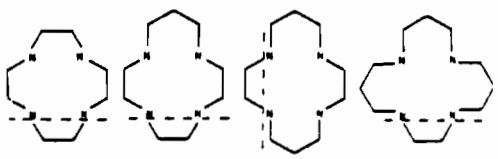			
	log $K_1(Cu^{2+})$			
open chain	20.1	23.2	21.7	17.1
macrocycle	23.3	24.4	26.5	24.4
	log $K_1(Zn^{2+})$			
open chain	12.0	12.8	11.3	9.4
macrocycle	16.2	15.6	15.5	15.0

[a] From: Martell, A. E.; Smith, R. M. "Critical Stability Constants Constants", First Supplement; Plenum Press: New York, 1982. The Cu(II) constants with the macrocycle are from: Thöm, V. J.; Hosken, G. D.; Hancock, R. D., submitted for publication. The broken lines indicate the bridging ethylene group to be removed from the macrocycle to generate the open-chain analogue. It is seen that the open-chain tetraaza polyamines show greater variation as the number of methylene groups in the ligand is varied than do the macrocyclic forms.

(1) Busch, D. H. *Acc. Chem. Res.* **1978**, *11*, 392.
(2) Thöm, V. J.; Fox, C. C.; Boeyens, J. C. A.; Hancock, R. D. *J. Am. Chem. Soc.* **1984**, *106*, 5947.
(3) Bosnich, B.; Poon, C. K.; Tobe, M. L. *Inorg. Chem.* **1965**, *4*, 1102.

0020-1669/85/1324-1208$01.50/0